

## Design of an Underactuated Origami Hand

Savannah Cofer, Becky Miller and Godson Osele

### Project Objectives:

1. **Explore** 3D printing of various flexible hinges
2. **Design** a 3D printable Sawhorse Voxel with the help of FEA analysis to identify failure modes
3. **Implement** our design in an underactuated origami hand consisting of the origami unit cells.



*Figure 1:* An underactuated 3D printed origami hand, including individual finger control and abduction/adduction of the fingers

### 1. Design Process:

The first step of our overarching design process was designing a model for a biomimetic robotic hand that could be created from voxel subunits. We identified the key motions of the hand being both a) underactuated flexion and extension of each of the fingers and b) abduction and adduction between the fingers. Based on our own hand, we measured the dimensions of each finger and the palm and the location of the thumb. We also studied the underactuated behavior of the curvature of the fingers, where a single tendon for each finger results in a complex motion.

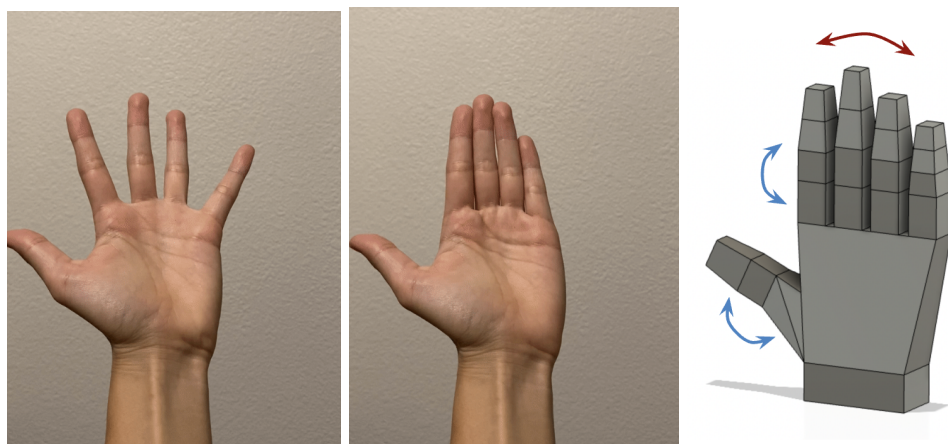


*Figure 2:* Constructing a CAD model based on the dimensions of the human hand that can be made from voxel shaped unit cells

After creating the voxel shaped hand, we converted each individual unit to a Sawhorse voxel origami pattern where the roll, pitch and yaw of the block matches the crease pattern on the unit cell. Using this inverse design process, we are able to enforce joint limits on the curvature of the finger that match the behavior of an actual human hand. For the abduction and adduction, we used a wedge shaped origami crease pattern to adjust the interstitial distance between the fingers.

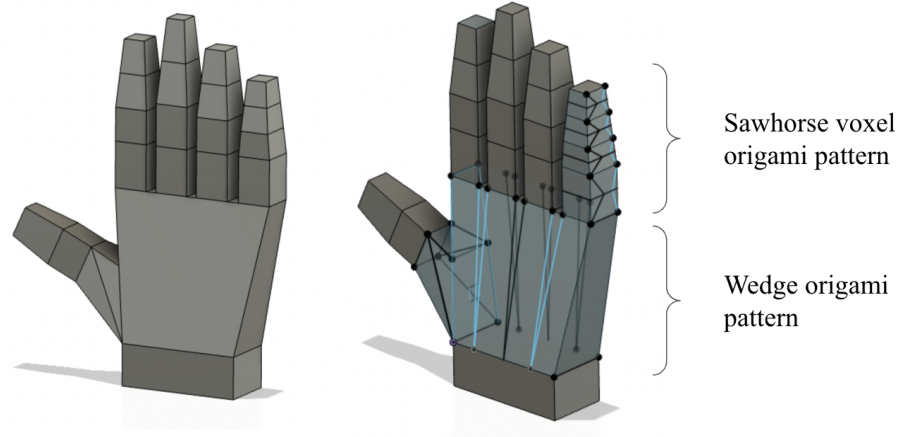


*Figure 3:* Converting the voxelized CAD model into an origami crease pattern

In our preliminary work, we show a Solidworks model of a single cube, which can be concatenated together with different vertex placements to create a robotic hand. Notably, this Solidworks model fails to buckle properly when 3D printed out of flexible resin as a test, showing the need for further optimization and development of origami hinges and placement of hinges for this particular crease pattern.

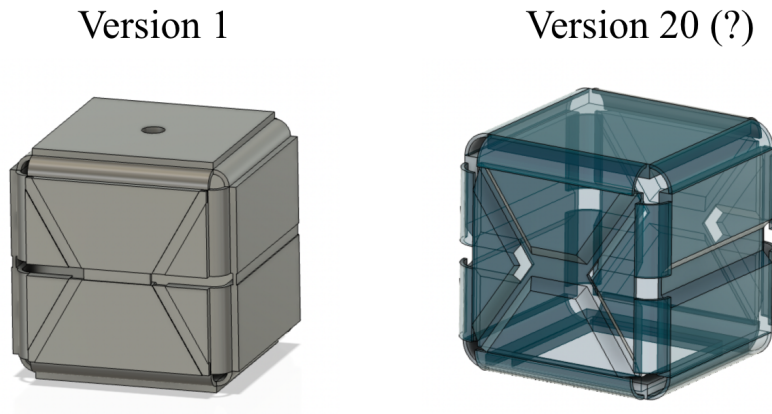


*Figure 4:* Comparison of design iterations for an individual Sawhorse voxel

In particular, we saw that the initial design tended to buckle outward when a compressive load was applied to the top. This effect was as a result of the design having the thin hinges fixed to the outer wall as opposed to the inner wall, as shown in Figure 5.

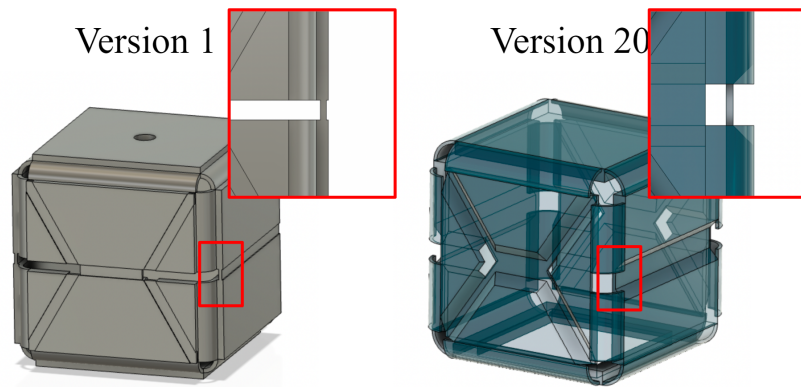


*Figure 5:* Highlighting a significant change in reversing hinge orientation

After reversing the orientation of the hinge, we started to see buckling inwards as desired. However, the buckling was minimal and we noticed that this was because the width of the thin hinge was not large enough in comparison to the thick sections. We subsequently increased the width of the thin hinge in comparison to the thick section. We demonstrate this difference in figure 5. To accommodate for increasing the hinge width while maintaining the original cube volume, we add chamfers along the edges (Figure 6). Lastly we wanted to address how cube handles stretch along the top and bottom from the coupled motion on the front face as the cube is compressed. To do this, we tried 3 different designs for the edges of the top and bottom face and observed how they responded to a compressive load applied to the top. In the end, we found option C (Figure 7) to be the best option as it resisted damages over several loading cycles. Options A and B exhibited tears over time. After determining the optimal design for a single cube, we then 3D printed multiple to concatenate together to finger digits

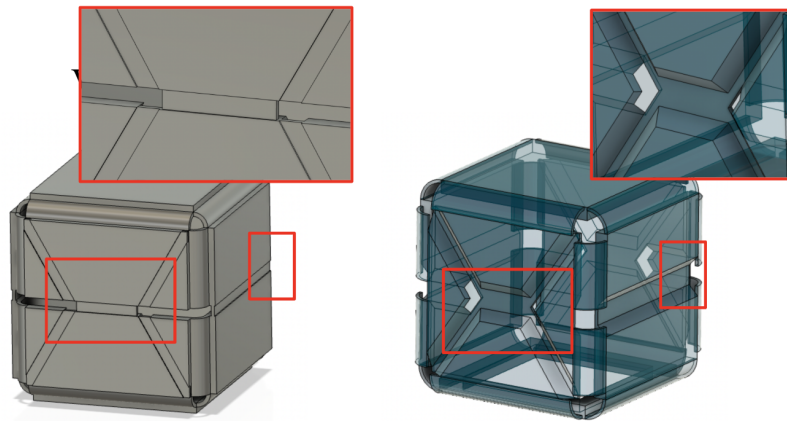


*Figure 6:* Highlighting design iterations of chamfers to the block along each internal face

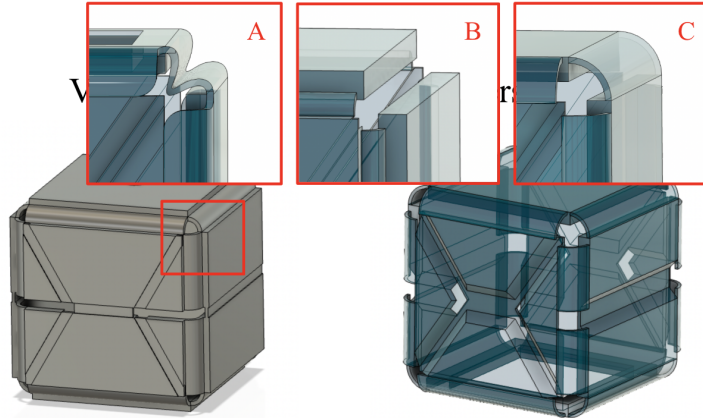


*Figure 7:* Handling “stretch” along the top corner of the block

Each finger consists of four blocks of varying heights, where the origami crease pattern is such that a roll motion is accomplished and can be propagated from block to block using a tendon driven movement. This is a novel design as the Sawhorse voxel shape has never been published in literature before, and we used inverse design to construct the crease pattern from a desired starting and ending configuration of the cube. Each finger had different dimensions and varying heights of the blocks according to the size of the finger.

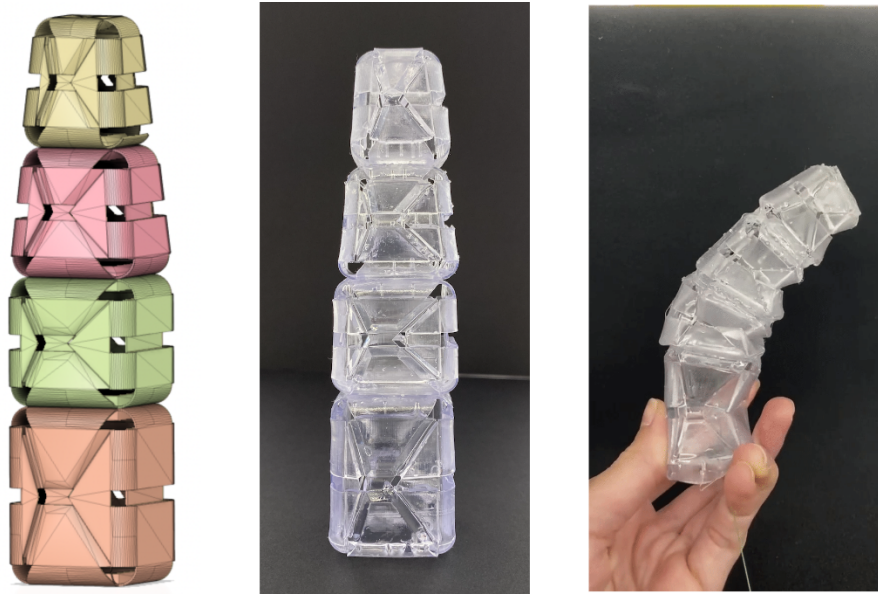


*Figure 8:* Design of an underactuated bending mode of a single index finger

As the palm of the hand had a significantly higher size than the individual digits and was unable to fit onto a 3D printed print bed, we used a combination of clear film and acrylic laser cut sheets to construct a wedge shaped origami pattern, as shown in Figure 8.

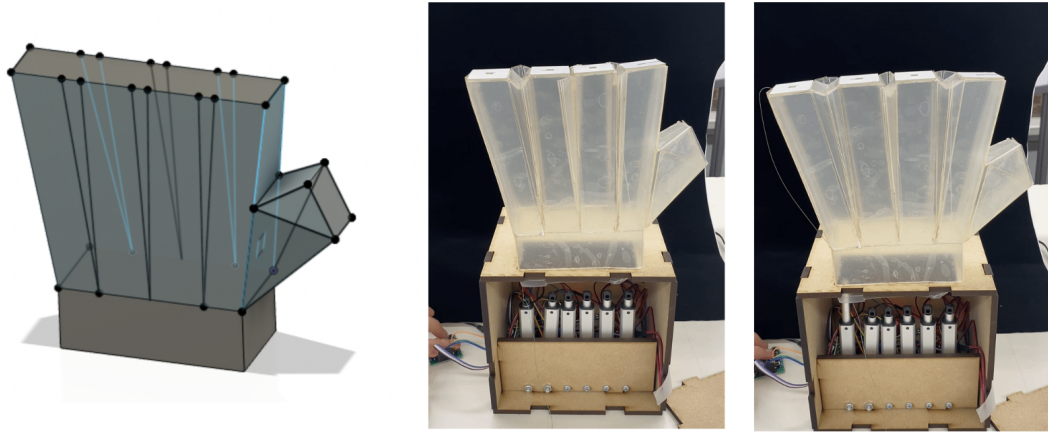


*Figure 9:* Design of a wedge origami mechanism to adjust the interstitial distance between fingers using a single tendon

## 2. Simulation process and challenges

Our goal with simulation was to use finite element analysis to identify high stress regions in the cube design and compare different types of 3D printed hinges. To do so, we run two FEA simulations applying 80 N of compressive force to the top of a single origami cube in tandem with the inward buckling of the side faces. One of the simulations uses a cube with a rounded hinge at the top and bottom faces while the other uses a hinge that has a fold in it (see figure 6). In both cases, we run one analysis with distributed force on the top face and then another with a concentrated force at the center node of the top face.

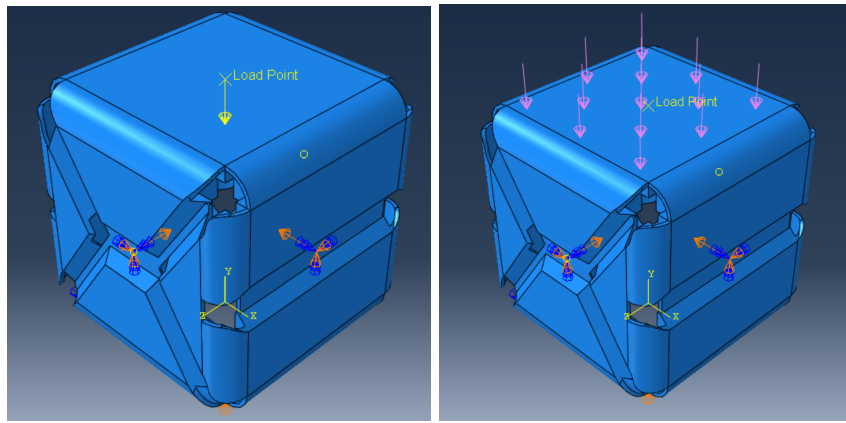


*Figure 10:* Distributed force vs. point load to the top block surface

Additionally, we set a boundary condition that fixes the bottom face of the cube to imitate it sitting on a flat surface and then another that displaces the side faces inward by 16.5 mm to simulate inward buckling. The displacement value is derived from the max displacement necessary to enter the next lowest energy configuration as determined by prior works in the development of the Sawhorse voxel.

For our 3D printing material, we use Flexible Resin 80A. To capture the right mechanical response in FEA, we tried four different methods to define the material properties. First, we tried just using the shear and young's moduli of EcoFlex 30 to see if we could get an expected general buckling response. This proved to be unhelpful as EcoFlex did not have a stiff enough response and led to failure as the compressive load led to the top surface folding inwards. We then tried to estimate the material properties using models from literature[1]. Unfortunately, both exhibited issues with convergence when we tried to run the analysis and given our limited amount of time, we decided to use tensile test data on the material collected by Dr. Cosima de Pasquier(a postdoc in the CHARM Lab working with the same material) to determine the material properties. We then proceeded to run the analyses as planned.

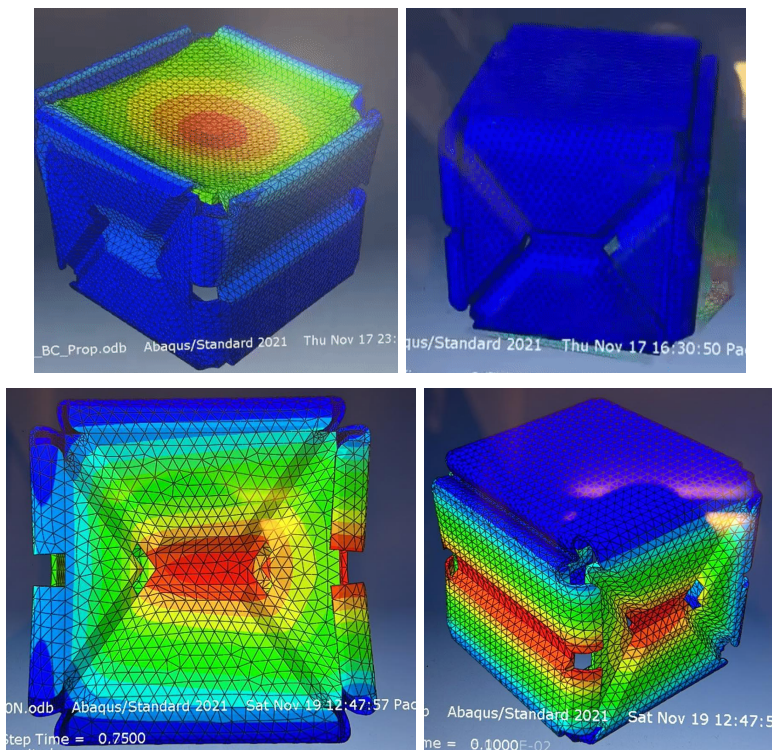
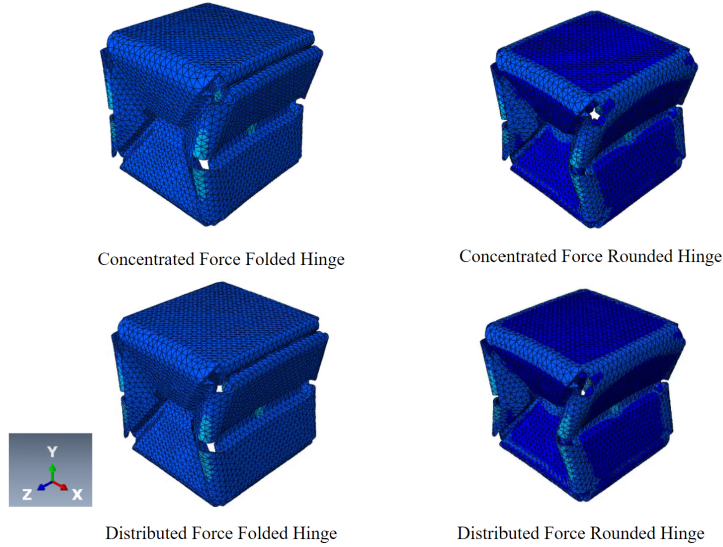


Figure 11: Failure mechanisms and challenges in the FEA modeling

We ran into a few more challenges. First we had to revisit the CAD model a few times as ABAQUS highlighted errors in the merging of solid bodies. Namely, the side hinges were disconnected and we were able to notice this after the FEA demonstrated failure at that point. This is seen in figure 11. After adjusting this, we saw the expected buckling response. A snapshot from the final results are seen below.



*Figure 12:* Comparison of folding behavior between rounded and folded hinges, and distributed and concentrated force application.

We also had to develop a low pass filter to post-process noisy field output data.

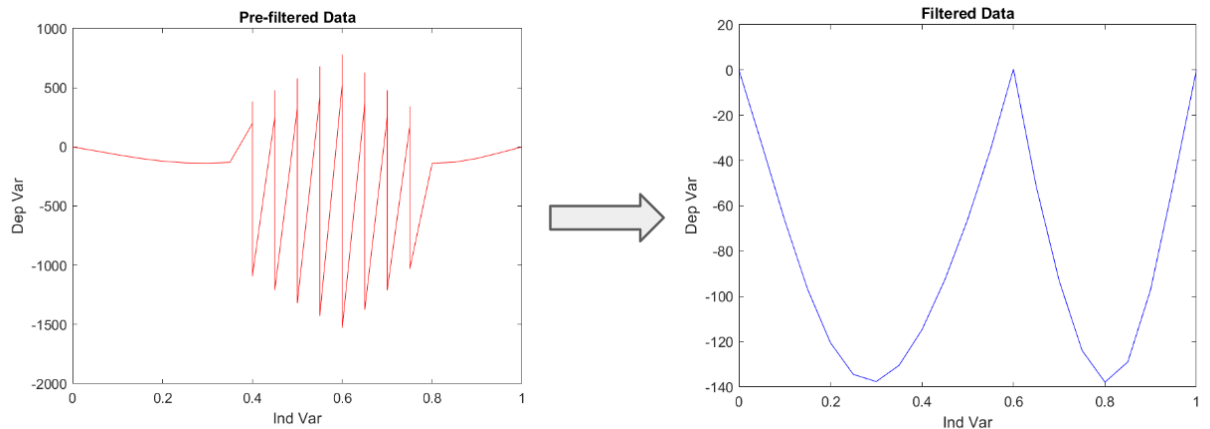


*Figure 13:* Low pass filter in MATLAB for post-processing output data

We collected data associated with the stress in the Top, Side and YZ Hinge and present it below. The main learning point was that the folded hinge along the top and bottom exhibited significantly less stress than the rounded hinge from the coupled motion on the front face as the cube is compressed.

This suggests that it would handle stretching best. However, in the process of fabrication, we found that the folded hinge was more susceptible to tears so we chose the rounded hinge as it was robust enough for our current application. We suspect this issue is moreso correlated to the curing of the print and once this is optimized, the folded hinge should resist tears better.

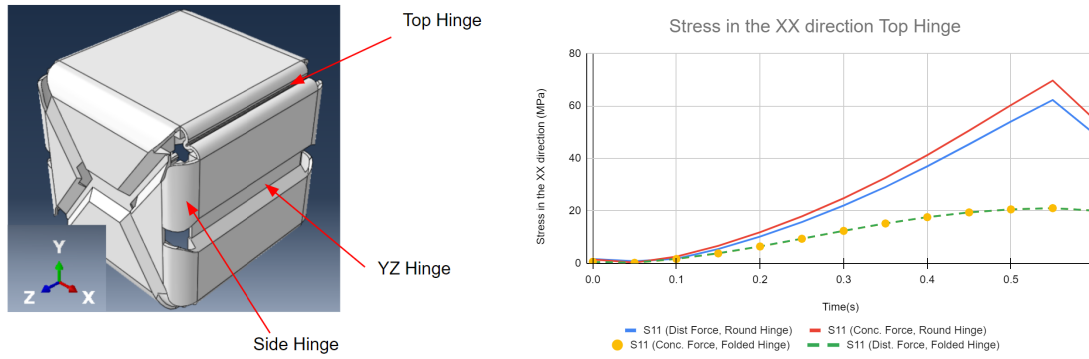


Figure 14: Hinge stress locations and stress plot in the XX direction

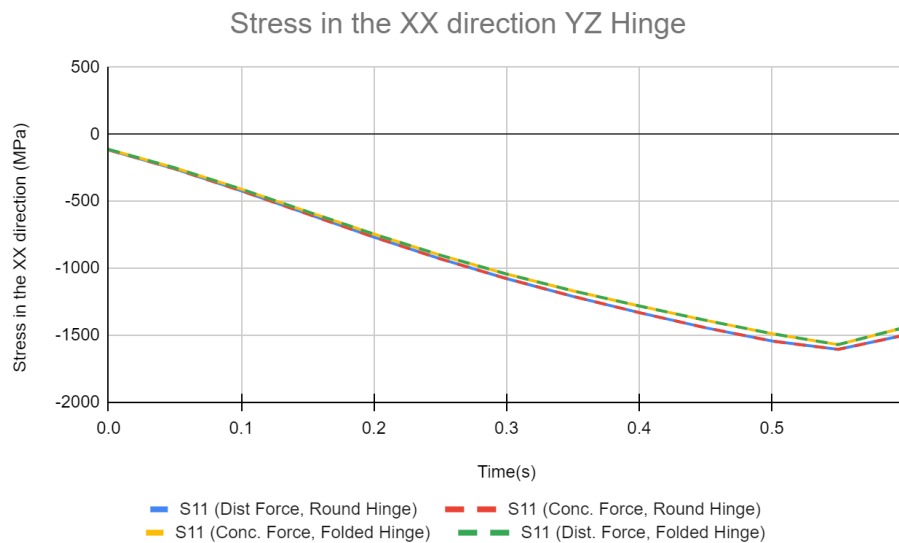


Figure 15: Stress plot in the XX direction for four types of block design

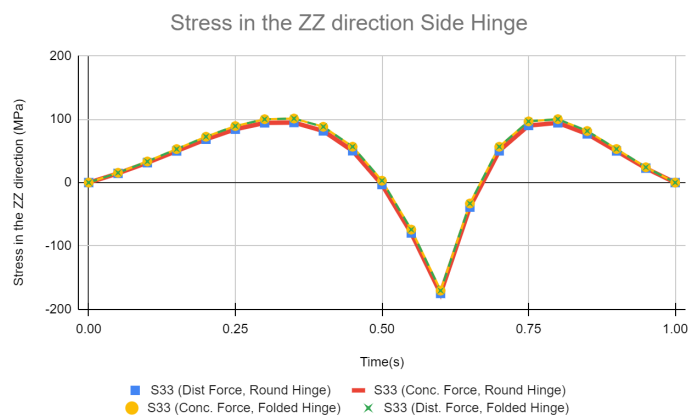


Figure 16: Stress plot in the ZZ direction for four types of block design

### 3. Fabrication method and challenges

This project focuses on the use of 3D printing of flexible material to construct foldable origami shapes. Although the Sawhorse voxel shape has previously been fabricated by a combination of rigid laser cut panels and flexible fabric sheets, the assembly process is time intensive and has failure modes when the flexible fabric delaminates from the rigid panels at high stress regions.



Figure 17: Laminate manufacturing methods used in prior work to fabricated the Sawhorse Voxel

Our first step of our design process was understanding the 3D printing process of various flexible hinges for both 180 degree and 90 degree hinges using the Flexible 80A resin of the Form3. By varying the thickness of the material throughout the part, we were able to localize the stress and strain creating a hinge that can take the place of the hinges created with the Lamine processes. We also experimented with removing more material in the hinge sections, but ultimately found that this resulted in a much weaker design and was not necessary to achieve the desired bending. We had also noted that when the rigid model was collapsed, gaps developed along some of the 90 degree hinges on the top and bottom surfaces because of the thickness of the rigid panels and the geometry of the folding. Anticipating that this hinge might need to stretch significantly to allow the voxel the full range of motion, we also developed various designs where the structure of the material along the hinge section allowed for large linear deformation as well as angular bending. Ultimately, we found that the simplest designs with an unbroken thin section along the desired fold line were most reliable and effective.

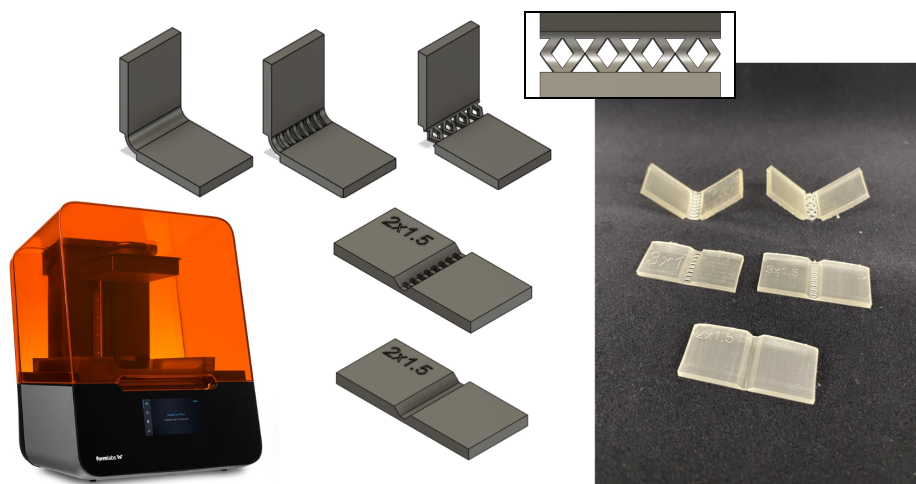


*Figure 18:* Fabrication of 3D printed 180 degree and 90 degree origami hinges

After understanding the hinge printing process, we began our process of design iterations. Figure 19 shows a few failure modes of the structure, including buckling outward, too-long curing time, breaking of voxel sides, and corner tearing. More information about the design side of this fabrication process is shown in Figures 4-7.

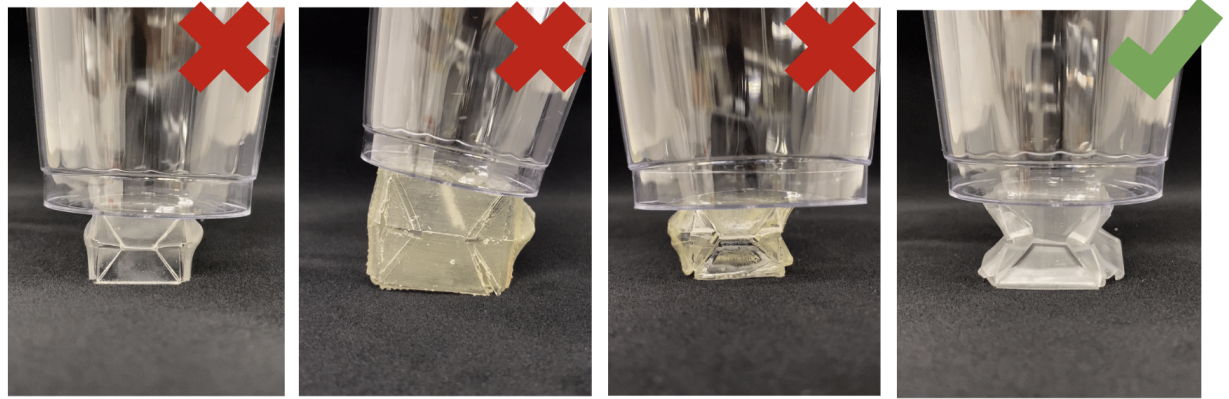


*Figure 19:* Fabrication challenges of different 3D printed origami voxel designs

After formulating a voxel shape that could be effectively fabricated and actuated reliably, we created a set of both parallel and angled blocks with varying dimensions to represent the index, middle, ring, and pinky fingers of the hand. The thumb design consists of two bendable voxels.



*Figure 20:* Fabrication of four finger digits of varying heights and angled components

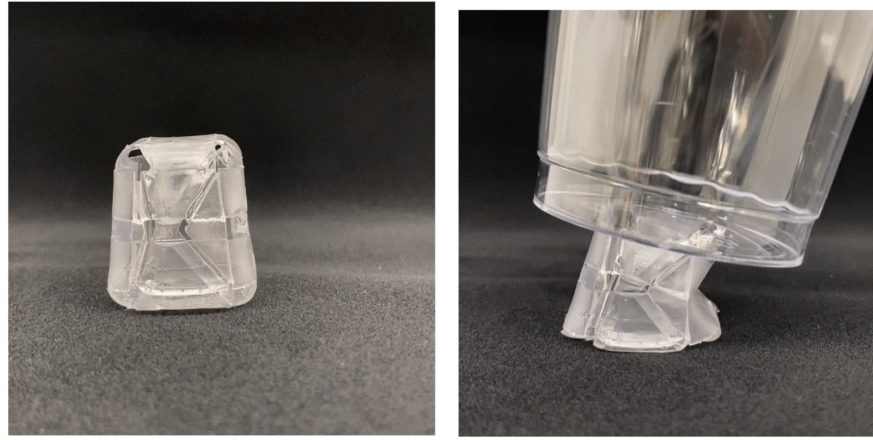


*Figure 21:* Fabrication of off-centered origami crease patterns that actuate to a bent end configuration, instead of a parallel end configuration.

#### 4. Actuation and performance evaluation

In this project, we use a tendon-driven actuation with an external array of linear actuators which causes the origami units to fold and create desired bend of fingers. This mimics the behavior of the actual human hand, which is a coupled system where finger position is controlled by long tendons moving along the length of the fingers. Each finger has a small rigid acrylic plate mounted to the upper surface of the top voxel. By attaching the tendon to this acrylic piece, the force is distributed across the top surface of the voxel, promoting the proper buckling mode. This design decision was informed by the FEA simulation results and manual testing of a single voxel. There are six linear actuators housed in the base of the hand that can independently control each of the five fingers, plus one to control the abduction and adduction of the hand. The elastic properties of the Flexible resin bias the fingers toward the unactuated position. Releasing the tension on the tendons allows them to return to this position in a controlled way.

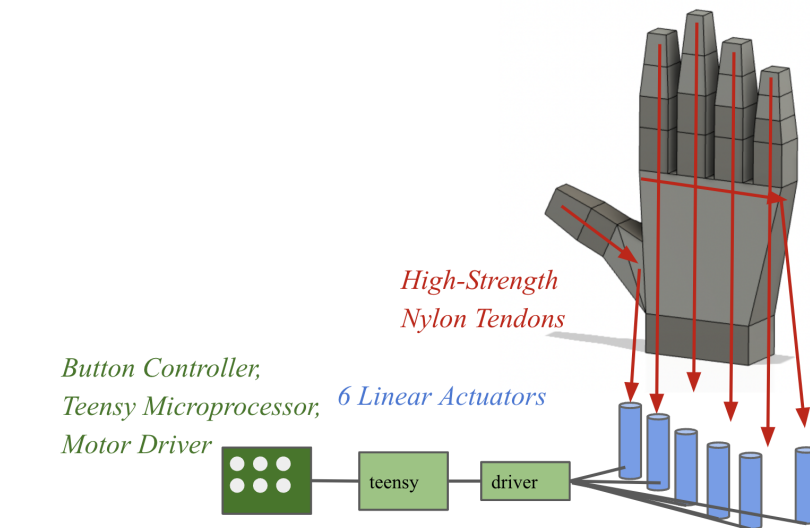


*Figure 22:* Schematic of tendon actuation system

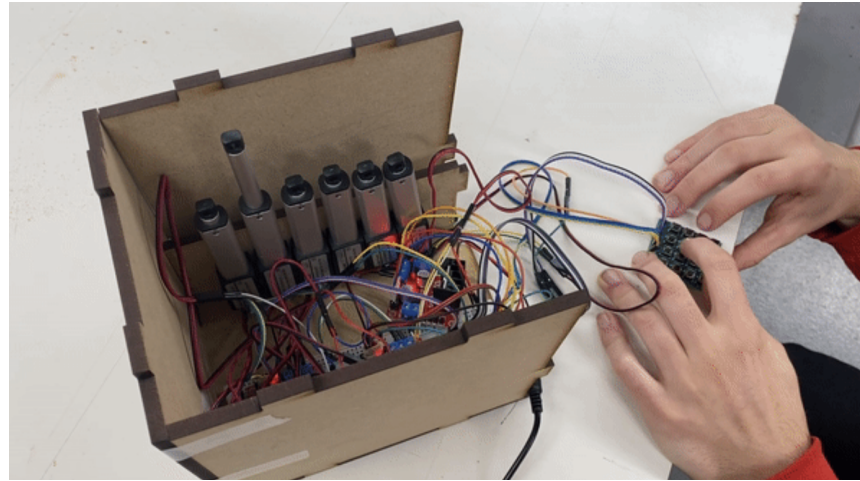


Figure 23: Linear actuators in fabricated actuation system, controlled by button pad

We validated our system with a series of videos showing successful hand motion, including underactuated behavior of each finger and the thumb individually, together, and the abduction and adduction of the fingers. We observed that the curvature of the hand matched the desired motion.



Figure 24: Unactuated vs Actuated Hand

Videos for visual validation of underactuated behavior are shown in our presentation at:  
<https://docs.google.com/presentation/d/1Vt22cpQ1eGeqfxakheRcdHKtIJj8vh6vI8qTtsB9pA/edit?usp=sharing>

## **Discussion and Conclusion**

Overall, we successfully demonstrated underactuated behavior using an origami soft robot with a novel structure of origami block, showing curvature and proper buckling behavior. FEA modeling also successfully matched the observed block behavior and pointed to insights regarding the strain and stress observed along individual hinges. While our characterization was limited to FEA, further analysis could include tensile testing of individual blocks or load cells in the hand mounted to each tendon. Another interesting insight is the energetic behavior of the blocks. Prior work in fabrication from paper or laminated rigid sheets demonstrated bistable behavior, with the block sitting in the buckled configuration after actuation, the 3D printed blocks were resilient to maintain their unfolded state after the stress concentration is released. This is an important design consideration in terms of fabrication, as blocks with a bistable behavior might be more desirable for reducing energy consumption while sitting in the end configuration, while blocks with a recovery behavior can be used for tendon actuation without a counter-elastic or a stiff rod.

1. <https://www.dow.com/content/dam/dcc/documents/en-us/tech-art/11/11-37/11-3716-01-durometer-hardness-for-silicones.pdf>